

## Beta-Decay Branching Ratio of the Lambda Hyperon\*

ROBERT P. ELY, GEORGE GIDAL, GEORGE E. KALMUS, LARRY O. OSWALD, WILSON M. POWELL,  
AND WILLIAM J. SINGLETON

*Lawrence Radiation Laboratory, University of California, Berkeley, California*

AND

FREDERICK W. BULLOCK, CYRIL HENDERSON, DAVID J. MILLER, AND F. RUSSELL STANNARD  
*University College London, London, England*

(Received 7 March 1963)

Lambda hyperons were produced by  $K^-$  mesons at rest in the Berkeley 30-in. heavy-liquid bubble chamber filled with a mixture of 76%  $\text{CF}_3\text{Br}$ –24%  $\text{C}_3\text{H}_8$  by weight. A search for the  $\beta$ -decay mode  $\Lambda \rightarrow p + e^- + \bar{\nu}$  was made. A total of 192 000  $\Lambda$  decays of the type  $\Lambda \rightarrow p + \pi^-$  was observed. Three methods of separating the  $\beta$ -decay mode from the mesonic decay and from other forms of background are discussed. The most successful method of calculating the branching ratio  $r = (\Lambda \rightarrow p + e^- + \bar{\nu}) / [(\Lambda \rightarrow p + \pi^-) + (\Lambda \rightarrow n + \pi^0)]$  made use of the  $\Lambda_\beta$  decays identified by the electron's stopping or starting to curl up in the chamber; also,  $r$  was calculated from  $\Lambda_\beta$  decays in which the negative secondaries left the chamber. The nonmesonic nature of these secondaries was established either by  $\delta$  rays or by decay kinematics. The values of  $r$  obtained by the different methods all agree within the errors. The best value obtained is  $r = (0.82 \pm 0.13) \times 10^{-3}$ .

### INTRODUCTION

SOON after the discovery of parity nonconservation in weak interactions, Feynman and Gell-Mann<sup>1</sup> and Sudarshan and Marshak<sup>2</sup> proposed a successful theory of the weak interactions of nonstrange particles. Their straightforward extension of this theory to the beta decay of the lambda,

$$\Lambda \rightarrow p + e^- + \bar{\nu}, \quad (1)$$

predicts a branching ratio of 1.6%. Bubble chamber groups which had analyzed several thousand lambda decays soon realized that this ratio was an order of magnitude lower than that predicted.<sup>3</sup> Aubert *et al.*,<sup>4</sup> on the basis of 8 events, have recently reported a ratio  $(3.0_{-1.2}^{+1.5}) \times 10^{-3}$ .

This paper describes an experiment in which 150 beta decays were found among 192 000 visible lambdas.<sup>5</sup> The events have been separated into groups according to the method of identification, and a branching ratio is determined for each group.

Results on the angular correlations between the decay products and on the branching ratio of the muonic decay  $\Lambda \rightarrow p + \mu^- + \bar{\nu}$  will be presented in a later report.

\* Work done in part under the auspices of the U. S. Atomic Energy Commission.

<sup>1</sup> R. P. Feynman and M. Gell-Mann, *Phys. Rev.* **109**, 193 (1958).

<sup>2</sup> E. C. G. Sudarshan and R. E. Marshak, *Phys. Rev.* **109**, 1860 (1958).

<sup>3</sup> W. E. Humphrey, J. Kirz, A. H. Rosenfeld, J. Leitner, and Y. I. Rhee, *Phys. Rev. Letters* **6**, 478 (1961).

<sup>4</sup> B. Aubert, V. Brisson, J. Hennessy, P. Mittner, J. Six, C. Baglin, M. Bloch, A. Bressy, A. Lagarrigue, A. Orkin-Lecourtois, P. Rancon, A. Rousset, and X. Sauteron, in *Proceedings of the Aix-en-Provence International Conference* (Centre d'Etudes Nucleaires de Saclay, Seine et Oise, 1961), Vol. 1, p. 197.

<sup>5</sup> Preliminary results published in *Proceedings of the 1962 Annual International Conference on High-Energy Physics at CERN* (CERN, Geneva, 1962), p. 445.

### EXPERIMENTAL PROCEDURE

#### Exposure

The experiment was performed in the Berkeley 30-in. heavy-liquid bubble chamber.<sup>6</sup> The chamber was filled with a 76%–24% mixture, by weight, of  $\text{CF}_3\text{Br}$ – $\text{C}_3\text{H}_8$ . The large number of  $\Lambda$ 's necessary for this experiment was obtained from the reaction  $K^-$  (at rest) + nucleus  $\rightarrow \Lambda$  + fragments. The  $K^-$  mesons were obtained from the Bevatron by using the 800-MeV/c separated beam of Murray *et al.*<sup>7</sup> To obtain the largest number of low-momentum  $\Lambda$ 's, which give decay electrons that are easily detected, the particles in the beam were degraded with copper absorber to 550 MeV/c before they entered the chamber. They were further degraded to 440 MeV/c by a 1-in. copper plate placed inside the chamber 5 in. from the entrance. The chamber was in a 13-kG magnetic field.

The composition of the bubble chamber liquid was decided upon as a compromise between obtaining a reasonable accuracy in the determination of momenta and the necessity to distinguish electrons from pions and muons. To obtain the desired mixture, the amounts of Freon and propane used were weighed by subtraction from their containers. The composition was checked by measuring the density, in the gaseous phase, of a small sample of liquid extracted at operating conditions, and allowance was made for the expansion ratio. A check on the density was made by using it as a free parameter in the range-energy relations and by constraining the  $\Lambda$  mass to 1115.36 MeV. For this a sample of  $\Lambda \rightarrow p + \pi^-$

<sup>6</sup> W. M. Powell, W. B. Fowler, and L. O. Oswald, *Rev. Sci. Instr.* **29**, 874, (1958).

<sup>7</sup> P. Bastien, O. Dahl, J. Murray, M. Watson, R. G. Ammar, and P. Schlein, in *Proceedings of an International Conference on Instrumentation for High-Energy Physics, Lawrence Radiation Laboratory, University of California at Berkeley, 1960* (Interscience Publishers, Inc., New York, 1961).

in which both secondaries stopped was used. The properties of the mixture can be summarized as follows:

Properties of the C <sub>3</sub> H <sub>8</sub> -CF <sub>3</sub> Br mixture	
Percentage composition (by weight)	24% C <sub>3</sub> H <sub>8</sub> , 76% CF <sub>3</sub> Br
Operating temperature	37°C
Operating pressure	283 lb/in. <sup>2</sup>
Density (under operating conditions)	0.89 g/cc
Radiation length	22.5 cm

The chamber was operated so that minimum-ionizing tracks contained 7 to 10 bubbles per cm in order to allow good ionization measurements. However, it was not possible to use ionization to distinguish electrons from pions because of the relativistic rise in electron-track bubble density. Gap-length measurements yielded 1.2 to 1.3×minimum ionization for 100-MeV/c electrons. This is to be compared to 1.2 to 1.5 for pions between 140 and 200 MeV/c, the most probable momentum range for those pions that did not stop in the chamber.

A total of 230 000 useful pictures was obtained with an average of about three *K*'s per picture. Two-thirds of the *K*'s stopped in the chamber, and the rest mostly interacted in flight. Approximately half the film was scanned and analyzed by each of the two participating groups.

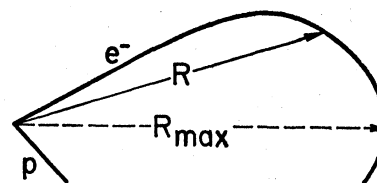
### Scanning Procedure

The entire film was scanned for both the mesonic decay,  $\Lambda \rightarrow p + \pi^-$ , and the beta decay,  $\Lambda \rightarrow p + e^- + \bar{\nu}$ . Events were required to have some possible origin in the liquid.

The identification of the mesonic-decay mode was established by comparing scan-table measurements of momenta, angles, and ionization with kinematic curves. All mesonic decays were recorded, but only those with a negative prong greater than 15 cm and leaving the chamber were measured on a digitized microscope or "Franckenstein." These latter events represented 2% of the total and were considered to be candidates for the beta-decay mode if they failed the kinematic-constraint program.

The more likely candidates for the β-decay mode were selected on the scanning table according to one of the following criteria: (a) The vector **R** from the point of

FIG. 1. The Δβ for which the vector **R** from the point of decay to a point along the track goes through a maximum value.



decay to a point along the track was seen to pass through a maximum value; such cases were noted as maximum-radius-vector (**R**<sub>max</sub>) events (Fig. 1). In 80% of these events the electron curled up and stopped in the chamber. (b) The negative track was greater than 15 cm in length, left the chamber, and had a δ ray greater than 1 cm, as measured on the scanning table. (c) The negative track left the chamber and was too long for a mesonic decay, as calculated from the proton momentum and the opening angle.

All the β-decay candidates were measured and rejected if the calculated mass was not consistent with the Λ mass. Measurements of the electron momenta were sufficiently uncertain so that this condition was primarily a test on the transverse momenta of the protons.

The first two columns of Table I list the number of events found by these procedures and the scanning efficiencies for each category. The scanning efficiencies were determined by comparing two independent scans. For the mesonic decay approximately 10% of the film was scanned twice, and the efficiency was found to be  $\epsilon_\pi = 0.89 \pm 0.01$ . To calculate  $\epsilon_\pi$ , we assumed that all the events had the same chance of being detected. This may not be true, however, for decay configurations in which the proton track was very short or in which the pion and proton were collinear. If these decay configurations were consistently missed, the scanning efficiency determined here would be too high. An upper limit to this bias is 3%.

For the β-decay candidates of the maximum-radius-vector variety, about 50% of the film was rescanned after the first scan was complete. To determine the efficiency of the second scan, each scanner was given film containing the events found by the others in the first scan. The average efficiency of both scans is  $0.87 \pm 0.05$ .

TABLE I. Numbers of events and branching ratios.

Category	No. observed	Scanning efficiency (%)	Estimated background (% observed)	Cutoff correction (%)	Detection efficiency (%)	Total	Branching ratio
Mesonic decay	192 000	89±1	<2	0	100±2	322 000±10 000	
<b>R</b> <sub>max</sub> 30° ≤ dip angle ≤ -30°	62	87±5	<3	90±3 <sup>b</sup> 50±0 <sup>c</sup>	60±2	265±40	(0.82±0.13)×10 <sup>-3</sup>
Delta rays <sup>a</sup>	12	67±15	17	94±2 <sup>d</sup>	7.1±1.5	224±100	(0.70±0.31)×10 <sup>-3</sup>
Kinematic events	17	90±7	10	47±4 <sup>e</sup>	18±4	200±70	(0.62±0.22)×10 <sup>-3</sup>

<sup>a</sup> Events are not included in these categories if they satisfy the **R**<sub>max</sub> condition.

<sup>b</sup> *l*<sub>p</sub> ≥ 2 mm and *l*<sub>e</sub> ≥ 9 cm.

<sup>c</sup> Dip angle between ±30°.

<sup>d</sup> *l*<sub>p</sub> ≥ 2 mm.

<sup>e</sup> Above line in Fig. 3.

The efficiency for finding  $\beta$  decays with  $\delta$  rays was determined by rescanning a sample of the film chosen so as to contain many of the events identified by  $\delta$  rays on the first scan. The average efficiency for  $\delta$  rays was found to be  $0.67 \pm 0.15$ .

In a similar fashion, the efficiency for finding  $\beta$  decays that did not obey mesonic  $\Lambda$  kinematics was estimated to be  $0.90 \pm 0.07$ .

### BACKGROUND

Because of the rarity of the type of event being studied, a thorough investigation of possible sources of background is necessary before the branching ratio can be determined. Later, it will be seen that attempts are made to obtain three independent estimates of the branching ratio from the three different methods of identification; some sources of background affect all categories, whereas others are important for only one of the methods.

The first source of background concerns very asymmetric electron pairs in which the positron is too short to be identified. This effect was eliminated completely by choosing a 2-mm cutoff length for the positive track.

Neutron interactions emitting a single proton and leaving the residual nucleus in a radioactive state that later  $\beta$  decays may also simulate leptonic  $\Lambda$  decays. The highest-energy electron expected from such a process is 13.6 MeV from the decay of  $B^{12}$ . In order that none of these events should be included, the electrons were required to have ranges of at least 9 cm. The measured  $\Lambda$ -momentum spectrum (Fig. 2) is used in a relativistic three-body phase-space calculation to correct for the proton and electron length cutoffs. The total correction is  $0.10 \pm 0.03$ . The error of 3% reflects the sensitivity of the laboratory-system momenta of the  $e^-$  and  $p$  to the nature of the matrix element for a  $V, A$  type of interaction, as well as the uncertainty in the  $\Lambda$ -momentum spectrum. This error might be somewhat larger for other types of interactions.

The next type of background concerns events in which the positively charged secondary leaves the chamber, so that it cannot be immediately identified as a proton. For these events there might be confusion between a  $\Lambda_\beta$  decay and a  $K_2^0$  decay, or a  $\mu^-$  entering the chamber

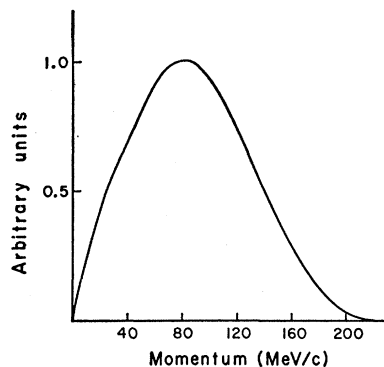


FIG. 2. Laboratory-system electron momentum spectrum obtained by folding  $\Lambda$ -momentum distribution (Fig. 3) into a three-body phase-space calculation

through the top or bottom glass and decaying into an electron near an origin. Fifteen events came into this category. These events could be identified as  $\Lambda_\beta$  decays on the basis of the ionization of the positively charged secondary.

Some neutron stars emit a proton and a  $\pi^0$  meson, and it is to be expected that a proportion of the  $\gamma$  rays from the  $\pi^0$  decays give asymmetric Dalitz pairs. The proton together with a negative electron from such a pair looks like a leptonic  $\Lambda$  decay. The chance of a positron's having an energy less than 0.3 MeV, and hence, passing unobserved, is about  $4 \times 10^{-3}$  for a  $\gamma$ -ray energy in the region of 80 MeV. Adding to this a  $1 \times 10^{-3}$  chance that the positron will annihilate in the first millimeter, the overall chance of missing the positron is  $5 \times 10^{-3}$ . Dalitz pairs from  $\pi^0$  decays occur with a frequency of 1 in 80, so the probability that such a neutron star will simulate a leptonic  $\Lambda$  decay is  $6 \times 10^{-5}$ . A search for electron pairs pointing back to proton recoils led to an estimated total of 200 neutron stars emitting  $\pi^0$  mesons. Thus, the contamination of background events is only 1 in approximately  $10^4$  leptonic  $\Lambda$  decays. Further possible confusion may arise when  $\gamma$  rays from the same source produce Compton electrons. A Compton electron may start within 1 mm of the star and so appear to have the same origin as the proton. From observations on Compton electrons pointing back to proton recoils, this background is estimated to be 1%.

Two further possible types of contamination are due to normal mesonic  $\Lambda$  decays for which the negative track contains a decay sequence  $\pi \rightarrow \mu \rightarrow e$ . The first type occurs when the  $\mu$  decays backwards in the  $\pi$  center-of-mass system and has so little energy in the laboratory system that it travels no detectable distance. This happens only for slow  $\pi$ 's. These have an ionization of at least 2.5 times minimum for a length of 1 cm before the decay point. This means that the change in ionization at the decay point is observable. The  $\pi$ 's decaying in less than 1 cm will not be so readily seen, but calculation showed the number of spurious events from these decays to be negligible. The second type of contamination occurs when the lines of flight of the  $\pi$  and  $\mu$  are opposite to that of the proton and seem to be a continuation of the proton track. When the angle between the proton and the  $\pi$  was restricted to be greater than  $170^\circ$  and the momentum of the  $\pi$  was restricted to be less than 45 MeV/c, the contamination due to this effect was calculated to be much less than one event in the film. Events falling outside these criteria could be easily recognized by the kink at the  $\Lambda$ -decay point and by the ionization of the  $\pi$ .

The sources of background outlined so far are expected to give less than two spurious leptonic  $\Lambda$ -decay events in the experiment.

The most important source of confusion affecting events identified solely by  $\delta$  rays is the fairly large number of stray Compton electrons in the chamber. We have calculated the probability that the first bubble of

such an electron will coincide with the pion from a normal  $\Lambda$  decay in such a way as to simulate a  $\delta$  ray. Examination of our subjective criteria for deciding whether or not a doubtful  $\delta$  ray is, in fact, attached to a track has enabled us to estimate the effective volume associated with a track within which the track of a stray electron must commence for a chance coincidence to be established. The average effective volume for pions with lengths exceeding 15 cm and leaving the chamber was found to be  $0.6 \text{ cm}^3$ . This is  $1.6 \times 10^{-5}$  the total volume of the chamber. An average of 35 Compton electrons was found per picture, so the probability that one of these pions has a simulated  $\delta$  ray is about 1 in 1800. Confirmation of this result came from scanning for simulated  $\delta$  rays on tracks of stopping pions,  $K$  mesons, and protons, where it was known that there could not be genuine  $\delta$  rays of the necessary energy. This investigation leads to a contamination of 17% among leptonic decays identified by the  $\delta$ -ray method.

The largest background for events selected by the kinematics method was due to those normal  $\Lambda$  decays for which the  $\pi$  decayed undetected into a  $\mu$  in flight, after which the  $\mu$  left the chamber. In order to calculate the size of this effect, a Monte Carlo computer program was written to simulate  $\Lambda(\pi \rightarrow \mu)$  events of this type. The background was found to be quite large and very sensitive to the scanning criteria. Thus, due to the difficulty in calculating the actual background in the selected kinematic-type events, another method of separation was used. In this method the  $\Lambda(\pi \rightarrow \mu)$  background was eliminated by demanding that the kinematic-event configurations cannot possibly be simulated by the  $\pi \rightarrow \mu$  anywhere along the  $\pi$  track. A background due to neutron stars that produced a proton and  $\pi^-$  and having a configuration satisfying the kinematics of a  $\Lambda_\beta$  decay still remained. Film was scanned for neutron stars simulating kinematic  $\Lambda_\beta$  decays not associated with acceptable origins. A lifetime cutoff was used to select these events. Geometric factors were then used to determine the background of neutron stars that would constrain to good  $\Lambda_\beta$  events, on the basis of transverse momentum and lifetime. This was found to be 1.7 events, i.e., 10% of the number of events in the category.

#### DETERMINATION OF THE BETA-DECAY BRANCHING RATIO

Because the three different means used to identify an event as  $\Lambda \rightarrow p + e^- + \bar{\nu}$  have different detection efficiencies, the branching ratio has been calculated separately in each case. In general, the procedure is to apply corrections to the number of events observed for scanning efficiency, for the scanning bias introduced by the application of the minimum cutoff-length requirements on the two decay secondaries, and for the effects of background. The probability that a  $\Lambda_\beta$  decay is detected by the particular method is then determined, and the total number of leptonic decays is calculated from the observed number.

The branching ratio  $r$  is defined here as the ratio of the number of  $\beta$  decays to the number of mesonic decays. By assuming that two-thirds of the mesonic decays go via the charged mode, the total number of mesonic decays in the experiment is found to be  $322\,000 \pm 10\,000$ .

#### Branching Ratio from $R_{\text{max}}$ Events

In order to determine a rate, it is necessary to estimate the total number of leptonic decays from the number seen with electrons passing through  $R_{\text{max}}$ . A Monte Carlo program was written to simulate the formation of electron tracks from  $\Lambda$  decays. These were tested to see how many satisfied the detection criteria. The program initiated its electrons from the coordinates of a random sample of 208 normal  $\Lambda$  decays found in the chamber. The direction of the  $e^-$  was randomized, since the pions from normal  $\Lambda$  decays showed no detectable correlations with any direction in the chamber. The energy with which the electron starts is chosen from an energy spectrum (Fig. 2) obtained by folding the  $\Lambda$ -momentum distribution of Fig. 3 into a phase-space electron-energy spectrum in the center-of-mass system. Six tracks of different energies and angles were initiated from each origin.

The tracks were generated in cells of 0.9-cm length. In each cell four effects were reproduced. Firstly, an energy loss due to collision was evaluated. Secondly, the magnetic bending corresponding to the momentum and dip angle was calculated. Random choices were then made of both multiple-scattering and bremsstrahlung energy loss. At the end of each cell a new energy, position, and direction were computed, and a further cell was begun. This was repeated until either (a) the energy dropped below 1.5 MeV and the particle was considered to have stopped, or (b) the track passed through  $R_{\text{max}}$ . The final energy of the electrons and the detection efficiency as a function of dip angle and of initial electron momentum were compiled and printed.

The theory used for collision loss was that of Sternheimer.<sup>8</sup> The radiation loss was calculated from Heitler's

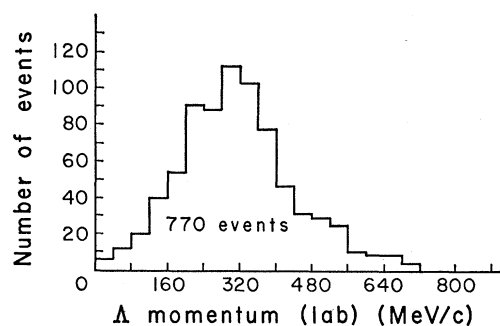


Fig. 3. Histogram of  $\Lambda$  momentum in the laboratory system.

<sup>8</sup> R. Sternheimer, Phys. Rev. **88**, 851 (1952).

analytic formula<sup>9</sup> by using the exact cross sections given by Koch and Motz,<sup>10</sup> and the multiple-scattering theory is that described by Barkas and Rosenfeld.<sup>11</sup>

Because of the numerous approximations involved in the theories, it was thought desirable to check the program against the behavior of a known sample of electrons. For this purpose  $\mu^-$  mesons that stopped in the chamber and decayed were used, inasmuch as they provided a source of electrons having a known energy spectrum. The coordinates of the origin, the initial direction of the electron, and the value of  $R_{\max}$  (where appropriate) were recorded for 170 of these  $\mu^-$  decays with all events accepted regardless of dip angle. It was observed that  $(62 \pm 6)\%$  of the electrons went through a maximum radius vector. The program predicted  $(65.5 \pm 2.5)\%$  by using the same origins and an electron spectrum given by the two-component neutrino theory ( $\rho = 0.75$ ).<sup>1</sup> The observed and calculated mean values of  $R_{\max}$  were 6.80 and 6.95 cm, respectively, and the shapes of the distributions of  $R_{\max}$  were found to agree well.

This confirmation of the accuracy of the program for electrons of energy less than 50 MeV was most satisfactory from the point of view of its application to the generally higher-energy electrons from  $\Lambda$  decay, since the main uncertainty in the calculation was in fact due to Heitler's approximation for bremsstrahlung below 40 MeV. Further confirmation came from runs of the program in which values of the radiation loss, collision loss, and magnetic field are changed by small amounts. Also, runs were made without multiple scattering. In every case the effect on the detection efficiency was small.

The value of the detection efficiency for  $R_{\max}$  events having negative secondaries with dip angle  $\leq 30^\circ$  was found to be  $0.60 \pm 0.02$ . The error arises predominantly from the statistics on the number of  $\Lambda$ -decay origins fed into the program, and also from the accuracy to which the  $\mu^-$ -decay run provides confirmation of the calculation. The dip-angle requirement was found to be necessary in practice because steeply dipping electrons that pass through  $R_{\max}$  can be confused with stopping pions.

The number of events detected by the  $R_{\max}$  criterion and satisfying the dip-angle requirement was 62. The scanning efficiency for this class of events was  $0.87 \pm 0.05$ . The correction of  $0.10 \pm 0.03$  also had to be applied for events excluded by the requirement that the range of the proton should be greater than 2 mm and that of the electron greater than 9 cm. The Monte Carlo program described here was used to obtain the part of this correction due to electron tracks that were too short. This contribution amounted to 4%. When these various factors are taken into account, the number of leptonic decays is estimated to be  $265 \pm 40$ . Dividing

this by the total number of  $\Lambda$  decays,  $322\,000 \pm 10\,000$ , gives the branching ratio  $r = (0.82 \pm 0.13) \times 10^{-3}$ .

### Branching Ratio from $\delta$ Rays

All negative secondaries leaving the chamber were examined for  $\delta$  rays. All events in which the  $\delta$  ray exceeded 1 cm were reported by the scanner. This cutoff was chosen because only about 1.5% of the  $\Lambda$ 's gave  $\pi^-$ 's capable of producing these  $\delta$  rays. For each event the proton momentum and the opening angle were used to calculate the pion momentum corresponding to mesonic  $\Lambda$  decay. Events in which this pion could have produced a  $\delta$  ray of the observed length were rejected.

Twenty events were found in which the electron did not also go through a maximum radius vector. There was good reason to believe that the scanning efficiency for  $\delta$  rays on tracks less than 15 cm long and leaving the chamber was very poor. The reason for this was that for events with negative secondaries longer than 15 cm a scan card had to be filled in by the scanner. This ensured that the track was looked at carefully and that the  $\delta$  ray was noted. For tracks less than 15 cm long the scanner did not have to record the fact that the track did not have a  $\delta$  ray, and thus many events possibly were missed. The total number of events with  $\delta$  rays and having negative tracks longer than 15 cm was 12. The total number of  $\Lambda\beta^-$ 's was calculated from these events by weighting each one according to the inverse of the probability that its electron should have produced a  $\delta$  ray satisfying the scanning criteria somewhere along its path length. The weighting factor for each event is  $[1 - \exp(-l/\lambda)]^{-1}$ , where  $l$  is the electron's path length and  $\lambda$  is the mean free path for producing that required  $\delta$  ray.

In practice, it was not possible to use the  $\delta$ -ray range in space, due to the heavy scattering suffered by low-energy electrons. Instead, the criterion has been to retain those events with negative secondaries that produce a  $\delta$  ray of projected length greater than or equal to 1.0 cm. Thus,  $\lambda$  in the above expression does not have its conventional meaning and is no longer simply calculated theoretically. It has been necessary, therefore, to determine the effective  $\lambda$  experimentally, and for this purpose we have scanned electron tracks from high-energy electron pairs. A value for the effective  $\lambda$  has been determined at several points throughout the run, since it has been found to vary with chamber sensitivity. This variation occurs because there is high probability of a scanner's judging the  $\delta$  ray to be a background Compton electron if its first bubble is separated by more than 2 or 3 mm from the parent track. The chamber sensitivity, as measured by the bubble density of minimum-ionizing tracks, is now related to the effective mean-free path. Once the bubble density on the picture concerned has been measured, the appropriate  $\lambda$  for any event is then available. Values of  $\lambda$  are typically about 37 cm.

The effective  $\lambda$  also varies with the velocity of the

<sup>9</sup> W. Heitler, *The Quantum Theory of Radiation* (Oxford University Press, London, 1957), 3rd ed., p. 378.

<sup>10</sup> H. W. Koch and J. W. Motz, *Rev. Mod. Phys.* **31**, 920 (1959).

<sup>11</sup> W. H. Barkas and A. H. Rosenfeld, Lawrence Radiation Laboratory Report UCRL-8030 Rev., 1961 (unpublished).

parent electron, and increases rapidly when the  $\gamma$  value of the electron drops below about 35. A procedure has been developed whereby the effective  $\lambda$  is suitably increased for those events having a stopped or nearly stopped electron.

A good check on the method is afforded by the  $R_{\max}$  electron events, since all  $R_{\max}$  electrons are positively identified by magnetic-field curvature. From the number of  $R_{\max}$  electrons with  $\delta$  rays, the method should be able to predict the number of  $R_{\max}$  electrons without  $\delta$  rays. It is calculated that from 29 events with  $\delta$  rays, there should be  $(69 \pm 14)$   $R_{\max}$  electrons altogether. There are, in fact, 79.

After 2.1 background events due to stray Compton electrons are subtracted, there are 9.9 events left with which to determine the  $\Lambda_\beta$  decay rate. These have an average weighting of about 2.5, which implies that about 40% of all  $\beta$  decays with a negative track leaving the chamber after 15 cm have a  $\delta$  ray. By means of the Monte Carlo program described previously, it is calculated that  $(18 \pm 4)\%$  of all  $\beta$  decays have such a length of negative track. Allowing, further, for 6% of all events lost because the proton range was less than 2 mm and for the scanning efficiency of  $0.67 \pm 0.15$ , the observed  $\delta$  ray events represent  $(4.4 \pm 1.5)\%$  of all  $\beta$  decays. On this basis the branching ratio is  $r = (0.70 \pm 0.31) \times 10^{-3}$ .

#### Branching Ratio from Kinematics

The kinematic events are required to have a negative track that leaves the chamber and is at least 15 cm long. In addition, a requirement is placed on the proton momentum and opening angle that eliminates all mesonic decays and retains a considerable fraction of the  $\Lambda_\beta$  decays. This defines a region in  $\Lambda_\beta$  decay phase space that cannot be simulated by normal  $\Lambda$  decays or  $\Lambda$  decays with a subsequent  $\pi \rightarrow \mu$  decay. This region is that above the line shown in Fig. 4. The line represents constant  $\pi$  momentum. The position of this line is determined by calculating the minimum initial momentum of a  $\pi$  which, by decaying into a  $\mu$ , can produce a 15-cm track. This pion momentum is 100 MeV/c.

In order to determine a branching ratio, the fraction of all  $\Lambda_\beta$  decays falling in this region was calculated by

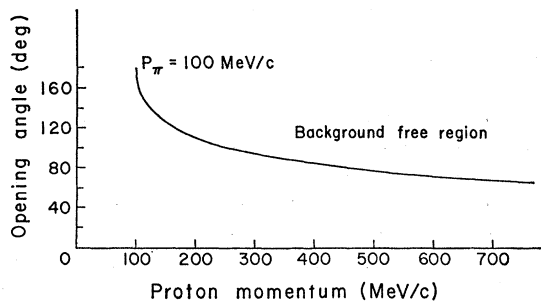


FIG. 4. Graph of opening angle between charged tracks versus proton momentum. Background from mesonic decays falls below line.

using a Monte Carlo program. The opening angle (between the proton and electron) and the proton momentum obtained from this program were plotted for each decay on a scatter diagram similar to Fig. 4. It was found that  $(0.47 \pm 0.04)$  of all  $\Lambda_\beta$  decays fell above the line. As explained in the section on  $\delta$ -ray events, it is estimated that  $0.18 \pm 0.04$  of all  $\Lambda_\beta$  decays have an electron length of 15 cm and leave the chamber before going through  $R_{\max}$ . The correction for this category due to the proton length cutoff of 2 mm is much less than one event. The scanning efficiency for these events is  $0.90 \pm 0.07$ . Seventeen events were found. A 10% correction is necessary for neutron-star background, leaving 15.3 events. These represent  $(7.6 \pm 2.7)\%$  of the total number of  $\Lambda_\beta$  decays in the film. From kinematic events the branching ratio is  $r = (0.62 \pm 0.22) \times 10^{-3}$ .

#### DISCUSSION

Because the electron-detection efficiency is not constant for all electron momenta, the branching ratio quoted depends on our assumption of the shape of the laboratory-system electron-momentum distribution. The electron-momentum distribution used is shown in Fig. 2. This was obtained by folding the  $\Lambda$ -momentum distribution (Fig. 3) into a simple three-body Lorentz-invariant phase-space calculation. Because of the insensitivity of the electron-momentum distribution to the nature of the matrix element for a  $V, A$  type of interaction, the branching ratios we obtain should hold within the quoted errors for this type of interaction.

From the detection-efficiency curves (Fig. 5) the branching ratio can be calculated for any given laboratory-system electron-momentum spectrum.

The branching ratios obtained by the  $R_{\max}$  and the  $\delta$ -ray and kinematic methods are in good agreement, in spite of the different shapes of the detection-efficiency curves. However, due to the large errors on the  $\delta$ -ray and kinematic ratios, not much can be inferred about the validity of the assumed electron-momentum spectrum, except that it is consistent with the results, and very large deviations from it are unlikely.

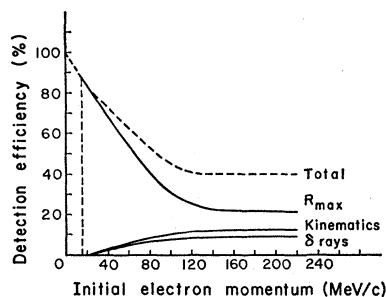


FIG. 5. Electron-detection efficiency curves for the three methods of identification. Dashed vertical line defines a 9-cm cutoff used for  $R_{\max}$  events. Total curve is slightly lower than the sum of the other three curves owing to a 10% overlap of kinematic and  $\delta$  ray events. A 100% scanning efficiency is assumed for all curves.

## CONCLUSION

The three determinations of the branching ratio are shown as follows:

- (a) Branching ratio from  $R_{\max} = (0.82 \pm 0.13) \times 10^{-3}$ ;
  - (b) branching ratio from  $\delta$  rays =  $(0.70 \pm 0.31) \times 10^{-3}$ ;
- and
- (c) branching ratio from kinematics =  $(0.62 \pm 0.22) \times 10^{-3}$ .

It should be noted that the events used to determine (a) are completely separate from those used to determine (b) and (c). Different parts of the electron-energy spectrum are sampled by the three categories. It can be seen that all the values agree within the errors.

The best value obtained from this experiment for the branching ratio is that obtained from  $R_{\max}$  events. The 15% error quoted contains both the statistical uncertainty and the errors on the scanning efficiencies. We feel that any systematic error would be considerably less than this.

The confirmation of the branching ratio from  $R_{\max}$  by the  $\delta$ -ray and kinematic methods, in spite of much larger uncertainties, is valuable because the only common link in determining the ratios is the Monte Carlo calculation of detection efficiencies. Formerly, the best

estimate of the ratio was that of Aubert *et al.*,<sup>4</sup> who found  $(3.0_{-1.2}^{+1.5}) \times 10^{-3}$  on the basis of 8 events. The value found in our work is clearly in disagreement with the prediction of  $16 \times 10^{-3}$  made by Feynman and Gell-Mann.<sup>1</sup>

## ACKNOWLEDGMENTS

The University College London group is indebted to J. Burren and his co-workers at National Institute for Research in Nuclear Science, Harwell, for the use of their programs and to G. A. Cooklin for his help in processing the data. We wish to thank all who assisted in the scanning, especially A. Common, C. Dodd, M. Esten, and W. Knight. The financial support of the Department of Scientific and Industrial Research is gratefully acknowledged.

The Lawrence Radiation Laboratory group is indebted to Howard White and his co-workers for measurements and data-reduction programs, and to G. Griffin and F. Schwarz for their work on the chamber. Major parts of the scanning were done by S. Bates, R. Gamow, B. Requiro, P. Weber, R. Williams, T. Woodford, and Professor Frank Oppenheimer and his group at Colorado.

Finally, we thank Dr. Edward J. Lofgren and the Bevatron crew for their help during the run.

## Unitary Impulse Approximation\*

LEONARD ROSENBERG†

*Department of Physics, University of Pennsylvania, Philadelphia, Pennsylvania*

(Received 15 March 1963)

With the aid of multiple scattering expansions, Blankenbecler's generalized unitarity relation is derived for a multichannel three-body potential scattering problem. A matrix representation of the scattering amplitudes is obtained in the form of Heitler's integral equation, with the  $\mathbf{K}$  matrix replaced by a matrix  $\mathbf{N}$ , so that generalized unitarity is automatically satisfied if  $\mathbf{N}$  has no physical cut in the total energy variable. A simple, physically reasonable, choice for  $\mathbf{N}$  leads to representations of the inelastic amplitudes which have the form of initial- (or final-) state interaction corrections to the impulse approximation. With the elastic amplitude given, no sums over three-body phase space appear. The elastic amplitude itself is obtained as the solution of an integral equation which sums all diagrams which are iterations of the basic impulse approximation diagram. It is explicitly demonstrated that the partial-wave amplitudes thus obtained must satisfy unitarity even when the impulse (or strip) approximation is nonunitary. A convergent iterative solution is presented which treats the effects of longer ranged forces first and should be appropriate for high-energy diffraction scattering. Rearrangement collisions are treated in a similar way.

## I. INTRODUCTION

IT has become increasingly clear that relativistic field theory and potential scattering theory display a number of interesting similarities, particularly when both are formulated in the language of dispersion relations. This has the consequence that new techniques

developed in the context of one theory can find expression in the other, thereby establishing a useful interplay. We are concerned here with the development of approximation techniques which take into account the effects of inelastic scattering processes. We have chosen as our model a three-body potential scattering problem in which an energetic particle is incident on a target consisting of two other particles in a bound state. The problem then is to determine the amplitudes for elastic, breakup, and rearrangement processes. The individual

\* Supported by the National Science Foundation.

† Address after 1 September 1963: Department of Physics, New York University, University Heights Campus, New York, New York.